

Occurrence of titanium dioxide nanoparticle in Taihu Lake (China) and its removal at a full-scale drinking water treatment plant

Zhiyuan Liu

Shanghai Municipal Engineering Design Institute Group Co Ltd

Min Rui

Shanghai Municipal Engineering Design Institute Group Co Ltd

Shuili Yu (✉ 8566liliu@tongji.edu.cn)



State Key Laboratory of Pollution Control and Resources Reuse, Tongji University, Shanghai, 200092, China <https://orcid.org/0000-0003-2773-9342>

Research Article

Keywords: Drinking water treatment, X-ray absorption spectroscopy, Titanium dioxide nanoparticle, Taihu Lake

Posted Date: March 19th, 2021

DOI: <https://doi.org/10.21203/rs.3.rs-266362/v1>

License:   This work is licensed under a Creative Commons Attribution 4.0 International License.
[Read Full License](#)

Version of Record: A version of this preprint was published at Environmental Science and Pollution Research on November 22nd, 2021. See the published version at <https://doi.org/10.1007/s11356-021-15775-5>.

Abstract

The occurrence of titanium dioxide nanoparticle (TNP), an emerging contaminant, in Taihu Lake of China was investigated. Ti was present at a concentration of 224 ± 59 $\mu\text{g/L}$ in the water source of east Taihu Lake. Approximately 0.19% of the Ti-containing matter was at the nano-scale. Scanning Electron Microscope analysis verified the existence of Ti-containing components, such as TiO_x and FeTiO_x . Furthermore, Ti K-edge X-ray absorption near-edge structure spectroscopy was used to detect the phase composition of nano-scaled Ti-containing matter. The spectra showed the three characteristic peaks of TiO_2 in the samples, suggesting the occurrence of TNP in Taihu Lake. A least-squares linear combination fitting analysis indicated that the TNP concentration in the water source was 0.86 $\mu\text{g/L}$, with a crystal composition of 0.44 ± 0.1 $\mu\text{g/L}$ amorphous, 0.14 ± 0.03 $\mu\text{g/L}$ anatase and 0.28 ± 0.06 $\mu\text{g/L}$ rutile. The removal performance of the TNP at a full-scale conventional drinking water treatment plant indicated that 58.8% of TNP was removed via coagulation/sediment, sand filtration and disinfection/clear water reservoir. The coagulation/sediment process accounted for approximately 76.6% of the total removed TNP. The finished water contained 0.33 $\mu\text{g/L}$ TNP with a crystal composition of 0.24 ± 0.13 $\mu\text{g/L}$ anatase and 0.09 ± 0.05 $\mu\text{g/L}$ rutile. This study is the first that reported the presence and transport of TNP in a drinking water treatment system.

Introduction

Engineered nanoparticles (ENPs) represent an important class of emerging contaminants due to their release into the environment (Gottschalk et al. 2015; Kiser et al. 2009; Mueller and Nowack 2008). Compared with the bulk counterpart, ENPs possess a significant difference in their physical and chemical properties (Nel et al. 2006), which stimulates the wide application of ENPs globally and results in their toxicity in the environment (Jomini et al. 2015; Yu et al. 2015). Titanium dioxide nanoparticle (TNP) is one of the most commonly produced ENPs and is extensively used in photovoltaic cells, cosmetics, catalysts, coatings and cleaning agents, plastics, dietary supplements, etc. (Weir et al. 2012). Most of the environmental risk assessments of ENPs report that TNP is one of the highest risk ENPs in the aqueous environment based on their toxicology data and the predicted environmentally relevant concentration (Gottschalk et al. 2015; Gottschalk et al. 2009; Mueller and Nowack 2008).

Taihu Lake is located in the core area of the Yangtze River delta in China. It is one of the most important water sources of the ambient cities, including Shanghai, Suzhou, Nanjing and Wuxi. Its drainage area is 36895 km^2 , accounting for 0.4% of the total area of China (Qiu et al. 2004). Taihu Lake supplies water to 2.9% of the population and provides more than 10% of the gross domestic production (GDP) in China (Bureau of Taihu Lake Basin 2013). However, in recent years, as the economy has developed, heavier pollution and the eutrophication of lakes has worsened, and the primary source of Taihu Lake pollutants is considered an accumulation of nutrient-rich sewage and agricultural runoff into the shallow lake (Guo 2007). A similar exposure pathway of TNP was proposed in previous studies (Gottschalk et al. 2015; Gottschalk et al. 2009; Mueller and Nowack 2008), which implied the presence of TNP in the lake along

with sewage and agricultural runoff. However, the status quo concentration of TNP in Taihu Lake remains unknown.

To determine the TNP concentration in the environment, the most commonly used method to date is exposure modeling (Gottschalk et al. 2015). For example, Mueller, N. C. et al. modeled the quantities of nano silver, TNP, and carbon nanotubes released in Switzerland using a life-cycle perspective and reported that their expected concentrations in water were 0.03–0.08, 0.7–16, and 0.5–0.8 ng/L, respectively (Mueller and Nowack 2008). However, the actual TNP concentration may be different from the modeled values due to its complicated transport behavior in the environment (Battin et al. 2009). Moreover, the models are always performed under the assumption that TNP are naturally non-existent in the environment, which does not agree with the facts (Grafe et al. 2014). For the direct detection of TNP in the environment, studies have adopted element quantification (Kiser et al. 2009; Weir et al. 2012). However, the total titanium concentration may overestimate the TNP amounts because of the coexistence of other Ti-containing compounds in the environment, such as ilmenite and titanium chloride (Gaillard et al. 2001; Grafe et al. 2014). X-ray absorption near edge spectroscopy (XANES) is a powerful tool to investigate the local coordination environment of most of the metals in the environment, which could distinguish the various compounds, even those possessing the same metallic element (Eley et al. 1986; Gaillard et al. 2001; Manceau et al. 2002). Based on the linear fitting of the characterized pre-edge peaks of Ti K-edge XANES spectra, Lee Y. et al. calculated the phase ratio of anatase to rutile for TNP mixtures (Lee et al. 2003). For environmental samples (wastewater and sediment), Tong T. Z. et al. reported credible Ti fitting results using standard substances containing anatase, rutile, brookite, amorphous TiO_2 and ilmenite (Tong et al. 2015b). Although their study did not focus on TiO_2 on the nano-scale, XANES was shown to be a useful technique to detect TiO_2 in the environment.

Drinking water treatment is one of the main strategies to prevent the ingestion of harmful contaminants, including ENPs, from an aqueous environment (Chalew et al. 2013). Conventional drinking water treatments typically involve coagulation/sediment, sand filtration and disinfection/clear water reservoir. The removal efficiency of ENPs using these technologies has been investigated extensively on the laboratory scale (Chalew et al. 2013; Hyung and Kim 2009; Li et al. 2013). However, the removal performance of ENPs during full-scale drinking water treatments is largely unknown.

In this study, the occurrence of TNP in the water source of east Taihu Lake was investigated via acid dissolution, size grading, inductively coupled plasma mass spectrometry (ICP-MS), scanning electron microscopy (SEM) and XANES. Furthermore, the removal performance of TNP at a full-scale drinking water treatment plant using the conventional treatments of coagulation/sediment, sand filtration and disinfection/clear water reservoir was also studied. Our study represents the first report of the presence and the transport of TNP in such environmental samples, providing new insights for assessing the potential risks of TNP to people via drinking water system.

Materials And Methods

Sampling protocol

The water source (WS: 31°1' 20"N/120°26'40"E) is located in east Taihu Lake, serving as the water source for the Wujiang Drinking Water Plant (WDP). WDP supplies more than 200 billion liters of drinking water per year and meets the water demands of approximately 420,000 households, using the conventional drinking water treatments, i.e., coagulation/sediment, sand filtration and disinfection/clear water reservoir (Fig. 1).

To investigate the occurrence of TNP, water samples were collected at the WS 16 times over a one-month sampling period (December 10, 2014 to January 11, 2015), at a depth of 50 cm under the water surface. Sediments of the WS (WSS) were also collected under the water sampling points (top 30 cm). Locations of the sites for water/sediment sampling relative to WDP were detailed in the supporting information (Fig. S1). To study the removal performance of TNP in the drinking water treatment plant, effluent from various stages of the treatments of WDP was randomly collected five times over another one-month sampling period (January 11, 2015 to February 15, 2015) (Fig. 1). The hydraulic retention time in the treatments was considered during the water sampling. For each sampling point, three replicates were collected. After sample collection, the samples were sealed in glass bottles and stored below 4 °C until analysis.

Sample pretreatment

To investigate the acid solubility of the Ti-containing matter, the water samples were injected with HCl and HNO₃ to achieve the pH value of 2 and then centrifuged at 24149 g (12000 rpm) for 30 min (Jouan KR25i, Thermo Fisher Scientific, USA) to obtain the supernatant. The Ti concentration in the supernatant was then determined to evaluate the acid solubility of the Ti-containing matter. To evaluate the size fractionation of the Ti-containing matter, the water samples were treated with ultrasonication and then filtered through 0.1, 0.45, 0.8, 1.2, 5 µm PTFE membranes (Millipore, UK Ltd.) using a vacuum filtration device (Xinghua Glass Instrument Plant, Zhengzhou, China). To prepare the samples for XANES analysis, 100 L of each water sample was centrifuged at 24149 g (12000 rpm) for 30 min to obtain the concentrate (Jouan KR25i, Thermo Fisher Scientific, USA). Then, the concentrate was ultrasonically treated and filtered through a 0.1 µm PTFE membrane (Millipore, UK Ltd.) using vacuum filtration. The filtrate was centrifuged at 24149 g (12000 rpm) for 30 min. After the supernatant was discarded, the obtained sludge was dried for 12 h at 75 °C, which is a condition that does not alter the phase composition according to a previous study (Tong et al. 2015b). The dried sludge was stored in a drying oven until analysis.

The sediments were subjected to the same procedures as the water samples after being dissolved in ultrapure water for acid solubility, size fractionation and XANES analysis.

Titanium quantification

Titanium quantification was performed after chemical digestion. Briefly, an appropriate amount of samples (1 mL for raw water, 100 mL for the produced water) was dried on a plate digestion apparatus (DB-3EFS, Lichen Technology Co., LTD, China). Then, the samples were mixed with 5 mL mixtures (with a

weight ratio of 7:4 of sulfate: ammonium sulfate) and fired on the plate digestion apparatus at 300 °C for 30 min. Then, the mixtures were diluted to 50 mL with ultrapure water and analyzed via ICP-MS (Icap Q, Thermo Fisher Scientific, USA). The Ti recovery was $95 \pm 3\%$ when 0.3 µg of nano-scaled anatase was spiked into 10 mL of the raw water. The lowest limit of detection was 0.15 µg/L.

XANES analysis

Ti K-edge XANES spectra were acquired at the BL14W1 XAFS beamline at the Shanghai Synchrotron Radiation Facility. Ilmenite (FeTiO_3) (catalog no. 400874), Anatase (catalog no. 232033), Rutile (catalog no. 224227), Brookite (catalog no. 791326), and Amorphous TiO_2 were adopted as the standards to represent the components of Ti-containing matter in the samples. Amorphous TiO_2 was synthesized in the laboratory according to the procedure described by Wang YD et al. (Wang et al. 2003), while the others were purchased from Sigma Aldrich Co., USA.

The dried sludge obtained from the samples was ground with lithium fluoride at a weight ratio of 1:10 due to the scarcity of the samples and then mounted on Kapton tape (DuPont) for XANES spectroscopy analysis.

The XANES spectra of all the standards were collected in the transmission mode using Oxford ionization chambers with 296-mm path lengths due to the high abundance of Ti (> 10%), while the spectra of the environmental samples were determined in the fluorescence mode using a germanium array detector. During the measurement, the synchrotron was operated at the energy of 3.5 GeV and a current between 150 and 210 mA. Background subtraction and edge normalization were performed using the Athena program (version 0.9.17). The TiO_2 concentration was calculated according to the method reported by Tong T. Z. et al. (Tong et al. 2015b). Briefly, Least-squares linear combination fitting (LCF) was performed from -30 to 80 eV relative to the absorption edge (4966.4 eV) to quantify Ti speciation. Then the TiO_2 concentration was calculated using the following equation.

$$\text{TiO}_2 \text{ concentration} = \frac{\text{Ti concentration} \times 79.87}{47.87 \times (1 - \text{ilmenite})} \quad (1)$$

Where 79.87 is the molecular weight of TiO_2 , 47.87 is the molecular weight of Ti, and ilmenite represents the percentage of ilmenite in the samples.

SEM analysis

The water samples were firstly filtered through a 5 µm [membrane](#) to remove the large impurities (Millipore, UK Ltd.). The filtrate was centrifuged for 30 min at 12000 rpm to obtain the sludge (Jouan KR25i, Thermo Fisher Scientific, USA). Then, the concentrate was digested using 50% hydrogen peroxide for 20 min to remove the organic matter. The mixtures were rinsed twice using ultrapure water and dried on a 0.22 µm [membrane](#) for SEM analysis at 20 kV (FEI Company, USA).

Results And Discussion

Occurrence of TNP in the water source in east Taihu Lake

As shown in Fig. 2, the Ti concentration in WS substantially shifted during the sampling period, achieving an average Ti concentration of $224 \pm 59 \mu\text{g/L}$ during the sampling period. The Ti concentration in sediments was relatively stable ($0.70 \pm 0.06 \text{ mg-Ti/g-dry}$). Similarly, a few studies have reported the Ti concentration in natural water and sediment. Tong, T. Z. et al. reported the Ti concentration in the sediment of a North Shore Channel in Skokie (USA) as $1.98 \pm 0.04 \text{ mg-Ti/g-dry}$ (Tong et al. 2015b), and from < 5 to $15 \mu\text{g/L}$ Ti in the effluent of a wastewater reclamation facility (Kiser et al. 2009). Thus, the Ti concentration in the water of Taihu Lake is significantly higher than the previously reported values, whereas the Ti concentration in sediment is similar. Principle component analysis (PAC) revealed the close correlation of Ti and turbidity (Fig. S2), indicating Ti in water may present in the state of colloid or suspended solids. Accordingly, the high contents of Ti in Taihu Lake is much likely due to the hydraulic disturbance of the sediment as the average depth is merely 1.9 m (Yang et al. 2008).

Taihu Lake from December 10, 2014 to January 11, 2015.

To estimate the presence of TiO_2 in the samples, the acid-dissolved fraction was determined, according to Fig. S3. It was found that the major fraction of Ti-containing matter in both WS and WSS could not be dissolved in HCl, implying that the main component of the Ti-containing matter was present as acid insoluble matter, such as TiO_2 , FeTiO_3 , $\text{Ti}(\text{OH})_3$ and Ti_2O_3 . Interestingly, HNO_3 could not decrease the insoluble Ti percentage as much as HCl could in the samples, implying the presence of the Ti-containing matter, which could be oxidized to a species that is insoluble in acid, such as TiO . After being decomposed by an ultrasonic treatment, the size fractionation of Ti-containing matter in water and sediment of the water source was performed (Fig. 3). The main Ti-containing matter in WS and WSS was present in the $> 5 \mu\text{m}$ fraction (approximately 77.3% for WS and 86.2% for WSS). The Ti concentrations between $0-0.1 \mu\text{m}$ in size in WS and WSS were $0.49 \pm 0.62 \mu\text{g/L}$ and $0.57 \pm 0.17 \mu\text{g/g-dry}$, respectively. This result confirmed the presence of nano-scaled Ti-containing matter in WS and WSS. SEM analysis confirmed the presence of TiO_x and FeTiO_x in WS. Most of the Ti-containing particles are present in the μm size, whereas some Ti-containing particles are aggregates of nano-scaled particles as shown in (Fig. S4).

As shown in Fig. 4, the spectra of WS and WSS show the three characteristic peaks in the pre-edge (labeled by the imaginary lines) and the characteristic shapes after edge (Fig. 4a). The three peaks are due to the Ti 4p-Ti 3d hybridization and Ti 4p-O 2p hybridization in TiO_2 , suggesting the presence of TiO_2 in the samples (Lee et al. 2003). Therefore, XANES further confirmed the presence of TNP in the water and sediment of east Taihu Lake.

According to the general estimation of the Ti-containing matter of east Taihu Lake in the above experiments, as well as the previous fitting results of Ti-containing matter in the environment (Tong et al.

2015b), we chose Ilmenite (FeTiO_3), Anatase, Rutile, Brookite, and Amorphous TiO_2 as the standards to represent the components of Ti-containing matter in the samples. The XANES spectra of the Ti reference compounds, on which the linear combination fitting (LCF) was based, are shown in the supporting information (Fig. S5). LCF was performed from -30 to 80 eV relative to the absorption edge (4966.4 eV) to quantify Ti speciation, and the data and results of the curve fitting are presented in Fig. 4b and Table S1. The best LCF yielded 0.00054 , 0.0007 , 0.00047 , 0.00056 and 0.0036 for the R-factor for WSS, WS and the samples collected after coagulation/sediment, sand filtration and the effluent of WDP, respectively. The goodness of fit reported by the R-factor further provides substantial evidence for the presence of TNP in the samples.

Combined with the Ti concentration on the nano-scale, the TNP concentration in the WS and WSS was calculated using Eq. 1. The TNP concentration in WS was 0.86 $\mu\text{g/L}$, with a crystal composition of 0.44 ± 0.1 $\mu\text{g/L}$ amorphous, 0.14 ± 0.03 $\mu\text{g/L}$ anatase and 0.28 ± 0.06 $\mu\text{g/L}$ rutile. The TNP concentration in WSS was 0.93 $\mu\text{g/g-dry}$, with a crystal composition of 0.31 ± 0.09 $\mu\text{g/g-dry}$ amorphous, 0.22 ± 0.07 $\mu\text{g/g-dry}$ anatase and 0.39 ± 0.12 $\mu\text{g/g-dry}$ rutile.

It was found that no brookite was detected in the water samples and sediment. The natural scarcity of Brookite and its poorer production due to the lack of proper usage compared with the other phases may be the primary reasons for this result (Allen et al. 2008). It can also be seen that the amorphous component accounted for a large fraction of the detected TNP in the water samples and sediment. Generally, amorphous TiO_2 has not been widely used in product applications due to its poor photocatalytic activity. Thus, amorphous TiO_2 may be a natural mineral. Similarly, approximately 24% of amorphous TiO_2 was present in the sediments of a river (Tong et al. 2015b). In addition, rutile and anatase were the main components in TiO_2 . Rutile is widely present in nature as a TiO_2 -containing mineral (Yu et al. 2013). Moreover, rutile has been massively produced for several decades. Similarly, anatase has a high photocatalytic activity and is used widely in products. Therefore, it is not surprising that rutile and anatase are detected in the samples. Previous studies reported similar environmentally relevant concentrations of TNP based on the exposure modeling. (Boxall et al. 2007; Gottschalk et al. 2009; Mueller and Nowack 2008).

Removal of TNP at the drinking water treatment plant

As shown in Fig. 5, significant fraction of both Ti and nano-scaled Ti was removed via coagulation/sediment (99.1% for Ti and 58.8% for nano-scaled Ti). The coagulation/sediment accounted for 61.5% in the total removed nano-scaled Ti. The removed fraction via sand filtration was 20.9%, whereas the disinfection/clear water reservoir removed 17.5% of nano-scaled Ti-containing matter. Additionally, the removal performance deteriorated as the size of the Ti-containing matter decreased. Similarly, Ti larger than 0.7 μm was well removed by a wastewater treatment plant in the USA, while the < 0.7 μm fraction was poorly removed and was present in effluents in concentrations ranging from < 5 to 15 $\mu\text{g/L}$ (Kiser et al. 2009). The effective removal of TNP during coagulation/sediment was also found in

the jar test ([Abbott Chalew et al. 2013](#)), and the electrostatic interaction was considered to be the main removal mechanism.

As shown in Fig. 4, all the spectra of the effluent at various stages at the drinking water plant contained the three characteristic TiO_2 peaks in the pre-edge of TiO_2 (Fig. 4a), which indicated the presence of TNP at the various stages at the drinking water plant. For the calculation, the influent Ti species was obtained using the data of the water source. Fig. 6 shows that the TNP concentration in the influent was $0.8 \mu\text{g/L}$, with a crystal composition of $0.41 \pm 0.05 \mu\text{g/L}$ amorphous, $0.13 \pm 0.02 \mu\text{g/L}$ anatase and $0.26 \pm 0.03 \mu\text{g/L}$ rutile, whereas the TNP concentration in the effluent was $0.33 \mu\text{g/L}$, with a crystal composition of $0.24 \pm 0.13 \mu\text{g/L}$ anatase and $0.09 \pm 0.05 \mu\text{g/L}$ rutile. Similarly, Niall O'Brien et al. predicted that the mean TNP concentrations for the local drinking water treatment schemes ranged from 44.1 to 1450 ng/L ([O'Brien and Cummins 2010](#)).

In addition, different removal performances for the various TiO_2 crystals were observed during the drinking water treatments. During coagulation/sediment, the removal performance decreased in the order of amorphous, rutile and anatase. Previous studies have reported the different characteristics of some types of TiO_2 crystals in the aqueous environment. For example, Xuyang Liu et al. showed that crystallinity and morphology are not influential factors in determining the stability of TNP suspensions; however, the differences in their chemical compositions, notably, the varying concentrations of impurities (i.e., silicon and phosphorus) in the pristine materials, determined the surface charge, therefore determining the sedimentation and aggregation of TNP in the aqueous phase ([Liu et al. 2011](#)). Thus, the different removal performances during coagulation may be caused by the varying surface charge of the TiO_2 crystals.

Sand filtration did not provide efficient TNP removal. Similarly, the batch isotherms revealed poor adsorption between quartz sand and TNP, and the quartz sand provided nearly zero retention of a 50 mg TiO_2 per one liter stream in a column experiment ([Rottman et al. 2013](#)).

In terms of exposure pathways to humans, TNP in drinking water is most likely to gain exposure via the gastrointestinal and skin routes ([Hagens et al. 2007](#); [Lomer et al. 2002](#)). Previous studies producing lethal and sub-lethal effects in animal toxicity tests revealed the toxicity thresholds of 5 g/kg for rat ([Wang et al. 2007](#)), 10 g/m^3 for *Daphnia magna* ([Lovern and Klaper 2006](#)), 1 g/m^3 for Rainbow trout ([Federici et al. 2007](#)) and 40 g/m^3 for Algae ([Hund-Rinke and Simon 2006](#)).

According to China's water specifications, the drinking water consumption amounts per person per day is 75-220 L ([Ministry of Construction of the People's Republic of China 2002](#)). The adsorption and accumulation rate of TNP in humans was assumed as 10%, according to a previous study ([O'Brien and Cummins 2010](#)). Therefore, the annual ingestion of TNP through drinking water per person is 26.5 mg when using the highest water consumption amount, which is several orders lower than the above-mentioned toxicity thresholds. Moreover, this intake concentration is 100 times smaller than the concentration to which humans are exposed orally through daily food (0.2–2 mg/kg body weight per day

of nano-TiO₂/E171 in U.S.) (Weir et al. 2012). Thus, exposure to drinking water is extremely unlikely to result in a nano-specific toxicological response (O'Brien and Cummins 2010).

However, the presence of TNP in the drinking water system may result in secondary pollutants. For example, when TNP is present in the biological treatment, e.g., biological activated carbon filter, it may affect the pollutant removal performance because of its eco-toxicity (Li et al. 2014). Additionally, TNP may exert an influence on the disinfection effectiveness due to its affinity for bacteria (Wei 2011). Furthermore, TNP could alter the potential biological uptake of heavy metal ions, such as arsenic and lead (Miao et al. 2015; Sun et al. 2009). The coexistence of different types of nanoparticles was also reported to alter the original toxicity of individual nanoparticles (Tong et al. 2015a). Thus, comprehensive assessment of potential TNP toxicity in the drinking water system still requires careful integration of complex physicochemical interactions between TNP and other components in water.

Conclusions

In this study, a comprehensive and systematic survey was performed to evaluate the occurrence of TNP in the water source of east Taihu Lake (China) and its removal performance at a conventional full-scale drinking water treatment plant.

In the water source, 0.86 µg/L TNP was determined with a crystal structure of 0.44 ± 0.1 µg/L amorphous, 0.14 ± 0.03 µg/L anatase and 0.28 ± 0.06 µg/L rutile. The drinking water treatments achieved TNP removal of 58.8%. Sand filtration and disinfection/clear water reservoir exhibited poor removal efficiencies, while coagulation/sediment achieved higher efficiencies, responding to approximately 76.6% of the total TNP removed. However, 0.33 µg/L TNP was detected in treated waters, although at trace levels, suggesting the incomplete removal of TNP through the conventional process. Additionally, further studies are required to evaluate the secondary pollutants caused by the presence of TNP in a drinking water system.

Declarations

Ethics approval and consent to participate

Not applicable

Consent to publish

Yes

Authors contributions

Zhiyuan Liu was responsible for the design and implementation of the experiment, while Shuili Yu and Min Rui participated in the discussion of the experimental direction.

Funding

This work was supported by “The National Major Project of Science & Technology Ministry of China (No. 2012ZX07403-001)” and “The National Major Project of Science & Technology Ministry of China (No. 2017ZX07101002-04)”.

Competing interests

Not applicable

Availability of data and materials

Yes

Acknowledgments

The authors would like to thank BL14W1 beamline (Shanghai Synchrotron Radiation Facility) for providing the beam time.

References

1. Abbott Chalew TE, Ajmani GS, Huang H, Schwab KJ (2013) Evaluating nanoparticle breakthrough during drinking water treatment. *Environ Health Persp* 121:1161–1166. doi:10.1289/ehp.1306574
2. Allen NS, Edge M, Verran J, Stratton J, Maltby J, Bygott C (2008) Photocatalytic titania based surfaces. *Environmental benefits Polym Degrad Stabil* 93:1632–1646. doi:10.1016/j.polymdegradstab.2008.04.015
3. Battin TJ, Kammer FVD, Weilhartner A, Ottofuelling S, Hofmann T (2009) Nanostructured TiO₂: Transport Behavior and Effects on Aquatic Microbial Communities under Environmental. *Conditions Environ Sci Technol* 43:8098–8104 doi. Doi 10.1021/Es9017046
4. Boxall AB, Chaudhry Q, Sinclair C (2007) Current and future predicted environmental exposure to engineered nanoparticles. Central Science Laboratory, Department of the Environment and Rural Affairs, London
5. Bureau of Taihu Lake Basin (2013) The comprehensive planning of Taihu River Basin (2012–2030). Bureau of Taihu Lake Basin
6. Chalew TEA, Ajmani GS, Huang HO, Schwab KJ (2013) Evaluating nanoparticle breakthrough during drinking water treatment. *Environ Health Persp* 121:1161–1166 doi. Doi 10.1289/Ehp.1306574
7. Eley DD, Pines H, Weisz PB (1986) *Advances in catalysis*, vol 34. Academic Press, Orlando
8. Federici G, Shaw BJ, Handy RD (2007) Toxicity of titanium dioxide nanoparticles to rainbow trout (*Oncorhynchus mykiss*): Gill injury, oxidative stress, and other physiological effects. *Aquat Toxicol* 84:415–430. doi:10.1016/j.aquatox.2007.07.009

9. Gaillard JF, Webb SM, Quintana JPG (2001) Quick X-ray absorption spectroscopy for determining metal speciation in environmental samples. *J Synchrotron Radiat* 8:928–930 doi. Doi 10.1107/S0909049500020963
10. Gottschalk F, Lassen C, Kjoelholt J, Christensen F, Nowack B (2015) Modeling Flows and Concentrations of Nine Engineered Nanomaterials in the Danish Environment. *Int J Env Res Pub He* 12:5581–5602. doi:10.3390/ijerph120505581
11. Gottschalk F, Sonderer T, Scholz RW, Nowack B (2009) Modeled Environmental Concentrations of Engineered Nanomaterials (TiO₂, ZnO, Ag, CNT, Fullerenes) for Different Regions. *Environ Sci Technol* 43:9216–9222 doi. Doi 10.1021/Es9015553
12. Grafe M, Donner E, Collins RN, Lombi E (2014) Speciation of metal(loid)s in environmental samples by X-ray absorption spectroscopy: a critical review. *Anal Chim Acta* 822:1–22. doi:10.1016/j.aca.2014.02.044
13. Guo L (2007) Ecology - Doing battle with the green monster of. *Taihu Lake Science* 317:1166–1166 doi. DOI 10.1126/science.317.5842.1166
14. Hagens WI, Oomen AG, de Jong WH, Cassee FR, Sips AJAM (2007) What do we (need to) know about the kinetic properties of nanoparticles in the body? *Regul Toxicol Pharm* 49:217–229. doi:10.1016/j.yrtph.2007.07.006
15. Hund-Rinke K, Simon M (2006) Ecotoxic effect of photocatalytic active nanoparticles TiO₂ on algae and daphnids. *Environ Sci Pollut R* 13:225–232. doi:10.1065/espr2006.06.311
16. Hyung H, Kim JH (2009) Dispersion of C(60) in natural water and removal by conventional drinking water treatment processes. *Water Res* 43:2463–2470. doi:10.1016/j.watres.2009.03.011
17. Jomini S, Clivot H, Bauda P, Pagnout C (2015) Impact of manufactured TiO₂ nanoparticles on planktonic and sessile bacterial communities. *Environmental Pollutution* 202:196–204. doi:10.1016/j.envpol.2015.03.022
18. Kiser MA, Westerhoff P, Benn T, Wang Y, Perez-Rivera J, Hristovski K (2009) Titanium Nanomaterial Removal and Release from Wastewater Treatment Plants. *Environ Sci Technol* 43:6757–6763 doi. Doi 10.1021/Es901102n
19. Lee YS, Lim HM, Kim SJ, Lee WJ, Cho DH (2003) Estimation of phase ratio for nano-sized TiO₂ powders by TiK-edge. *XANES Res Chem Intermediat* 29:783–791 doi. Doi 10.1163/156856703322601799
20. Li DP, Cui FY, Zhao ZW, Liu DM, Xu YP, Li HT, Yang XN (2014) The impact of titanium dioxide nanoparticles on biological nitrogen removal from wastewater and bacterial community shifts in activated. *sludge Biodegradation* 25:167–177 doi. DOI 10.1007/s10532-013-9648-z
21. Li Z, Hassan AA, Sahle-Demessie E, Sorial GA (2013) Transport of nanoparticles with dispersant through biofilm coated drinking water sand filters. *Water Res* 47:6457–6466 doi:DOI. 10.1016/j.watres.2013.08.026
22. Liu X, Chen G, Su C (2011) Effects of material properties on sedimentation and aggregation of titanium dioxide nanoparticles of anatase and rutile in the aqueous phase. *J Colloid Interface Sci*

363:84–91. doi:10.1016/j.jcis.2011.06.085

23. Lomer MCE, Thompson RPH, Powell JJ (2002) Fine and ultrafine particles of the diet: influence on the mucosal immune response and association with Crohn's disease. *P Nutr Soc* 61:123–130. doi:10.1079/Pns2001134
24. Lovern SB, Klaper R (2006) *Daphnia magna* mortality when exposed to titanium dioxide and fullerene (C-60) nanoparticles. *Environ Toxicol Chem* 25:1132–1137 doi. Doi 10.1897/05-278r.1
25. Manceau A, Marcus MA, Tamura N (2002) Quantitative speciation of heavy metals in soils and sediments by synchrotron X-ray techniques. *Rev Mineral Geochem* 49:341–428 doi. DOI 10.2138/gsrmg.49.1.341
26. Miao W, Zhu B, Xiao X, Li Y, Dirbaba NB, Zhou B, Wu H (2015) Effects of titanium dioxide nanoparticles on lead bioconcentration and toxicity on thyroid endocrine system and neuronal development in zebrafish larvae. *Aquat Toxicol* 161:117–126. doi:10.1016/j.aquatox.2015.02.002
27. Ministry of Construction of the People's Republic of China (2002) Urban life water consumption standard vol GB/T50331-2002. Beijing
28. Mueller NC, Nowack B (2008) Exposure modeling of engineered nanoparticles in the environment. *Environ Sci Technol* 42:4447–4453 doi:Doi 10.1021/Es7029637
29. Nel A, Xia T, Madler L, Li N (2006) Toxic potential of materials at the nanolevel *Science* 311:622–627. doi:10.1126/science.1114397
30. O'Brien N, Cummins E (2010) Nano-scale pollutants: fate in Irish surface and drinking water regulatory systems. *Hum Ecol Risk Assess* 16:847–872 doi :Pii 926163982
31. 1080/10807039.2010.501270
32. Qiu XH, Zhu T, Jing L, Pan HS, Li QL, Miao GF, Gong JC (2004) Organochlorine pesticides in the air around the Taihu Lake. *China Environ Sci Technol* 38:1368–1374. doi:10.1021/es035052d
33. Rottman J, Platt LC, Sierra-Alvarez R, Shadman F (2013) Removal of TiO₂ nanoparticles by porous media: Effect of filtration media and water chemistry. *Chem Eng J* 217:212–220. doi:http://dx.doi.org/10.1016/j.cej.2012.11.117
34. Sun H, Zhang X, Zhang Z, Chen Y, Crittenden JC (2009) Influence of titanium dioxide nanoparticles on speciation and bioavailability of arsenite. *Environmental Pollution* 157:1165–1170. doi:10.1016/j.envpol.2008.08.022
35. Tong T, Wilke CM, Wu J, Binh CT, Kelly JJ, Gaillard JF, Gray KA (2015a) Combined toxicity of nano-ZnO and Nano-TiO₂: from single- to multinanomaterial systems. *Environ Sci Technol* 49:8113–8123. doi:10.1021/acs.est.5b02148
36. Tong TZ et al (2015b) Spectroscopic Characterization of TiO₂ Polymorphs in Wastewater Treatment and Sediment Samples. *Environ Sci Tech Let* 2:12–18. doi:10.1021/ez5004023
37. Wang JX et al (2007) Acute toxicity and biodistribution of different sized titanium dioxide particles in mice after oral administration. *Toxicol Lett* 168:176–185. doi:10.1016/j.toxlet.2006.12.001

38. Wang YD, Ma CL, Sun XD, Li HD (2003) Synthesis and characterization of amorphous TiO₂ with wormhole-like framework mesostructure. J Non-Cryst Solids 319:109–116 doi. Doi 10.1016/S0022-3093(02)01956-7
39. Wei J (2011) Bacterial Toxicity of Xide Nanoparticles and their Effects on Bacterials Surface Biomolecules. University of Massachusetts
40. Weir A, Westerhoff P, Fabricius L, Hristovski K, von Goetz N (2012) Titanium dioxide nanoparticles in food and personal care products. Environ Sci Technol 46:2242–2250. doi:10.1021/es204168d
41. Yang M, Yu JW, Li ZL, Guo ZH, Burch M, Lin TF (2008) Taihu Lake not to blame for Wuxi'. s woes Science 319:158–158
42. Yu H, Pan J, Bai Y, Zong X, Li XY, Wang LZ (2013) Hydrothermal Synthesis of a Crystalline Rutile TiO₂ Nanorod Based Network for Efficient Dye-Sensitized Solar Cells Chem-. eur J 19:13569–13574. doi:10.1002/chem.201300999
43. Yu R, Fang X, Somasundaran P, Chandran K (2015) Short-term effects of TiO₂, CeO₂, and ZnO nanoparticles on metabolic activities and gene expression of. Nitrosomonas europaea Chemosphere 128:207–215. doi:10.1016/j.chemosphere.2015.02.002

Figures

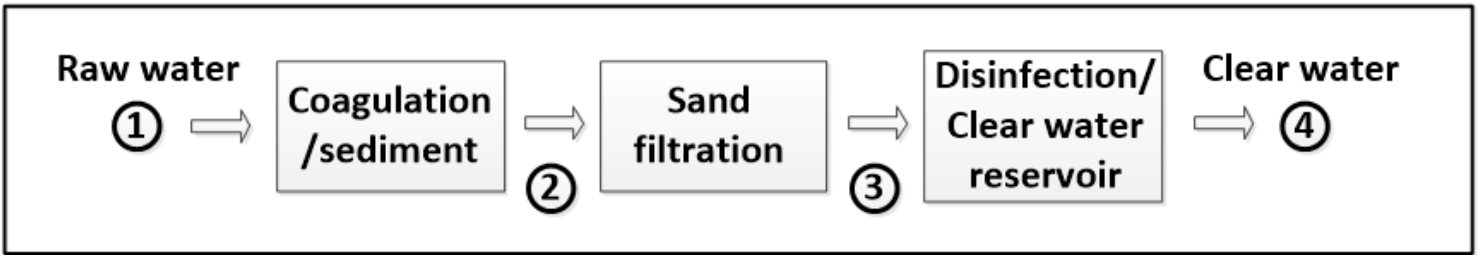


Figure 1

Treatment schemes of WDP. The numbers labeled between the treatments are the sampling points.
Sample pretreatment

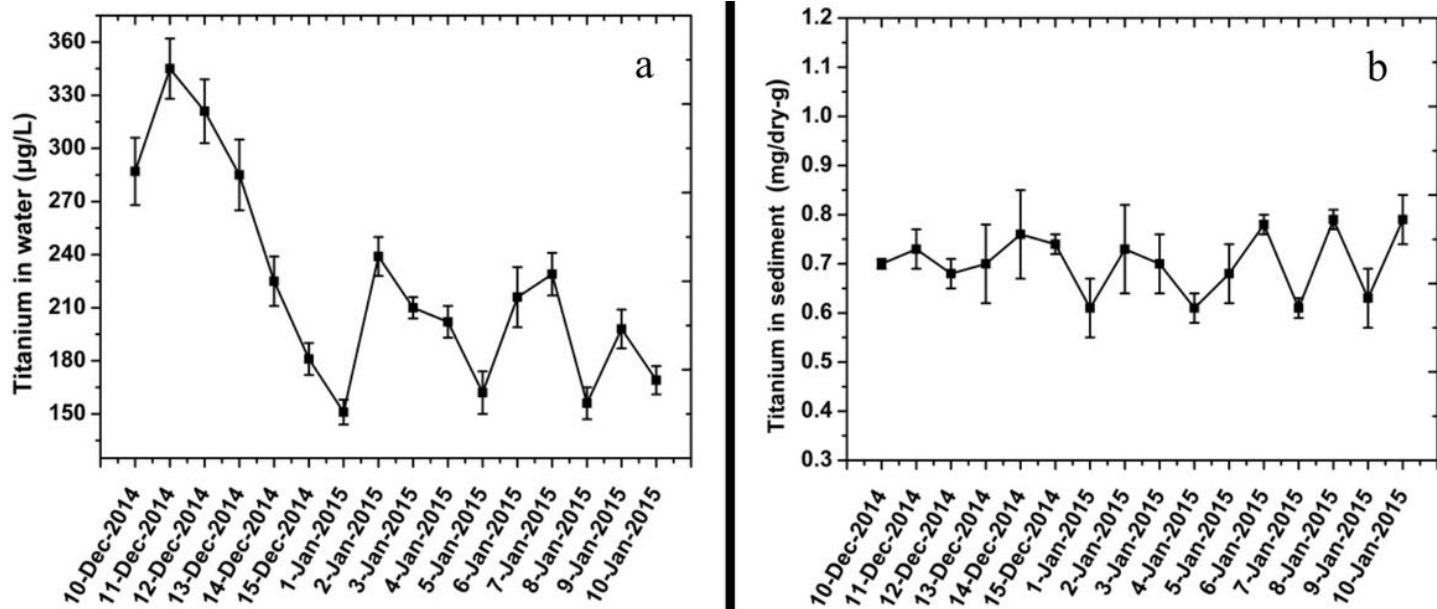


Figure 2

Ti concentrations in the water samples (a) and sediments (b) collected from the water source of east Taihu Lake from December 10, 2014 to January 11, 2015.

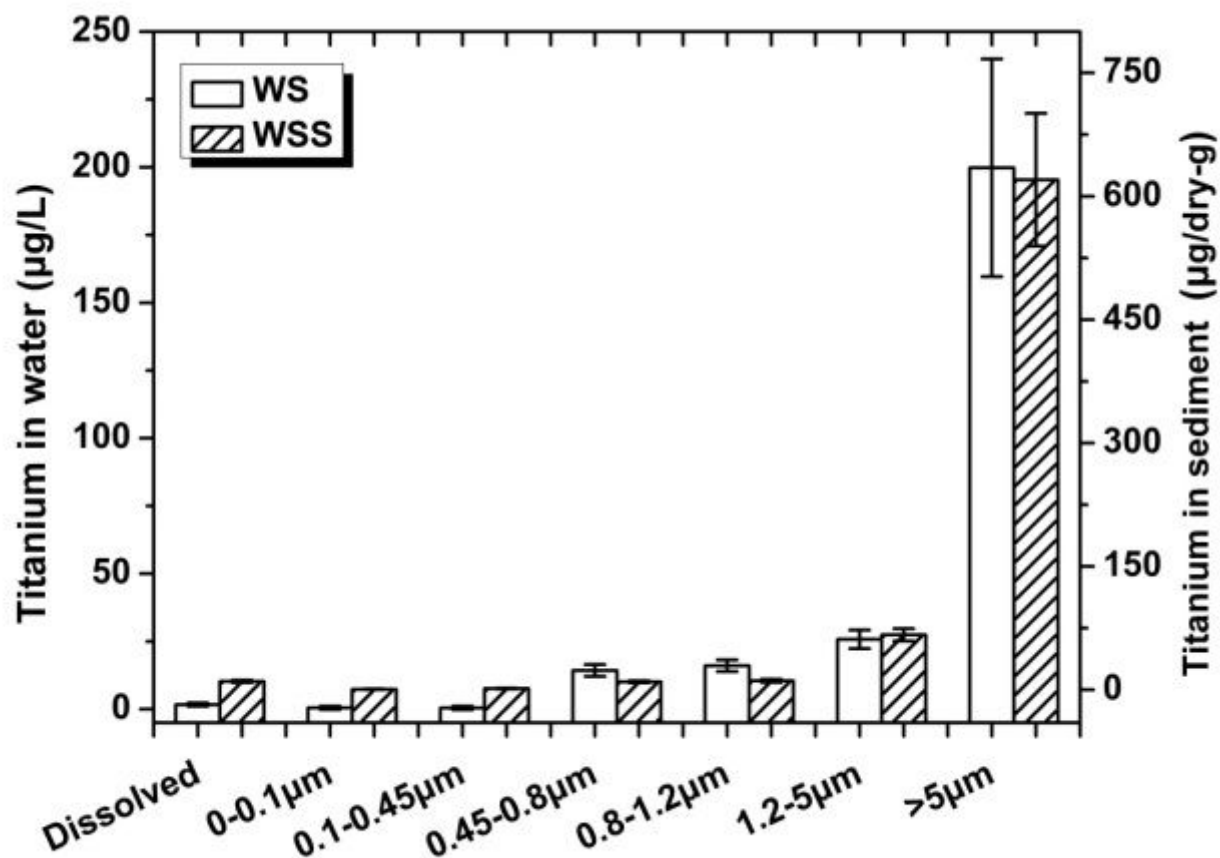


Figure 3

Size fractionation of Ti-containing matter in the water samples (left y-axis) and sediments (right y-axis) collected from the water source of east Taihu Lake. WS and WSS represent the representative water samples and sediments of the water source in east Taihu Lake, respectively.

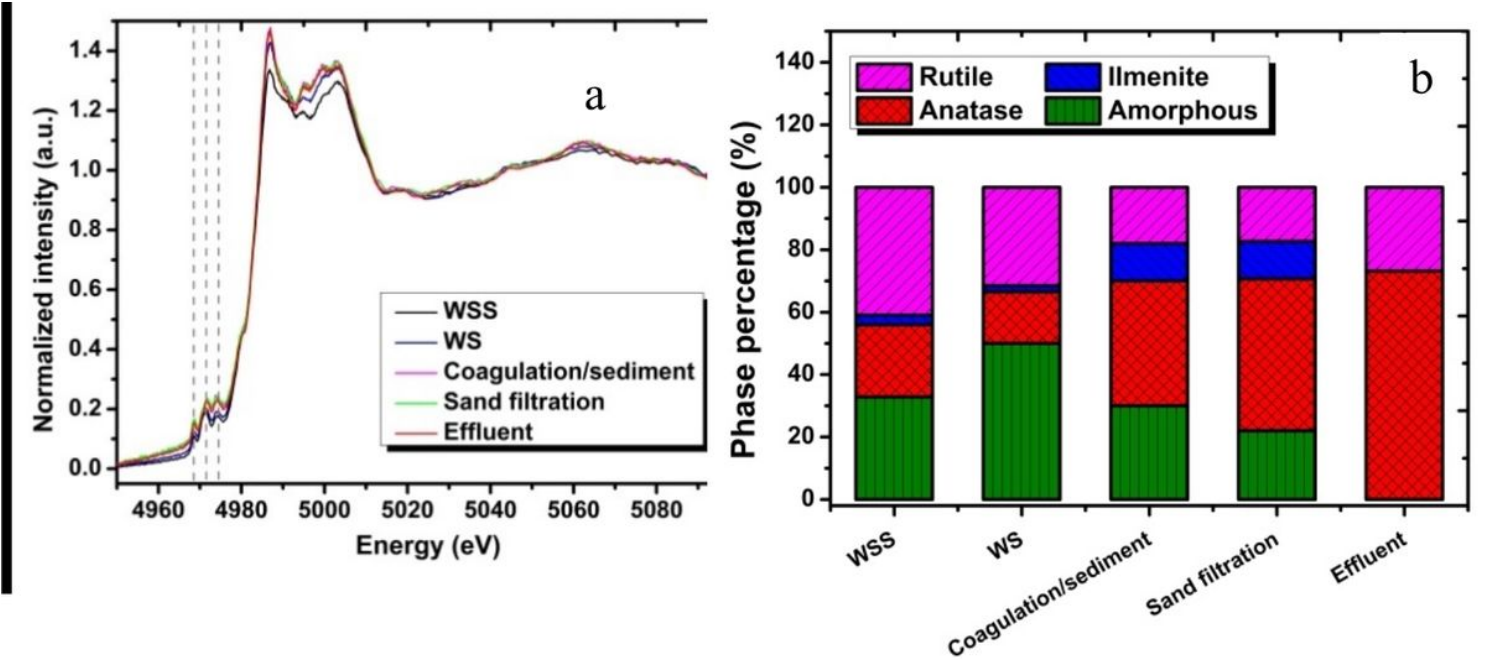


Figure 4

Normalized Ti K-edge XANES spectra (a), and the results of the linear combination fits (b) of Ti-containing matter (< 100 nm) in the representative water samples and sediment collected from the water source in east Taihu Lake or the effluents after various stages at the drinking water treatment plant.

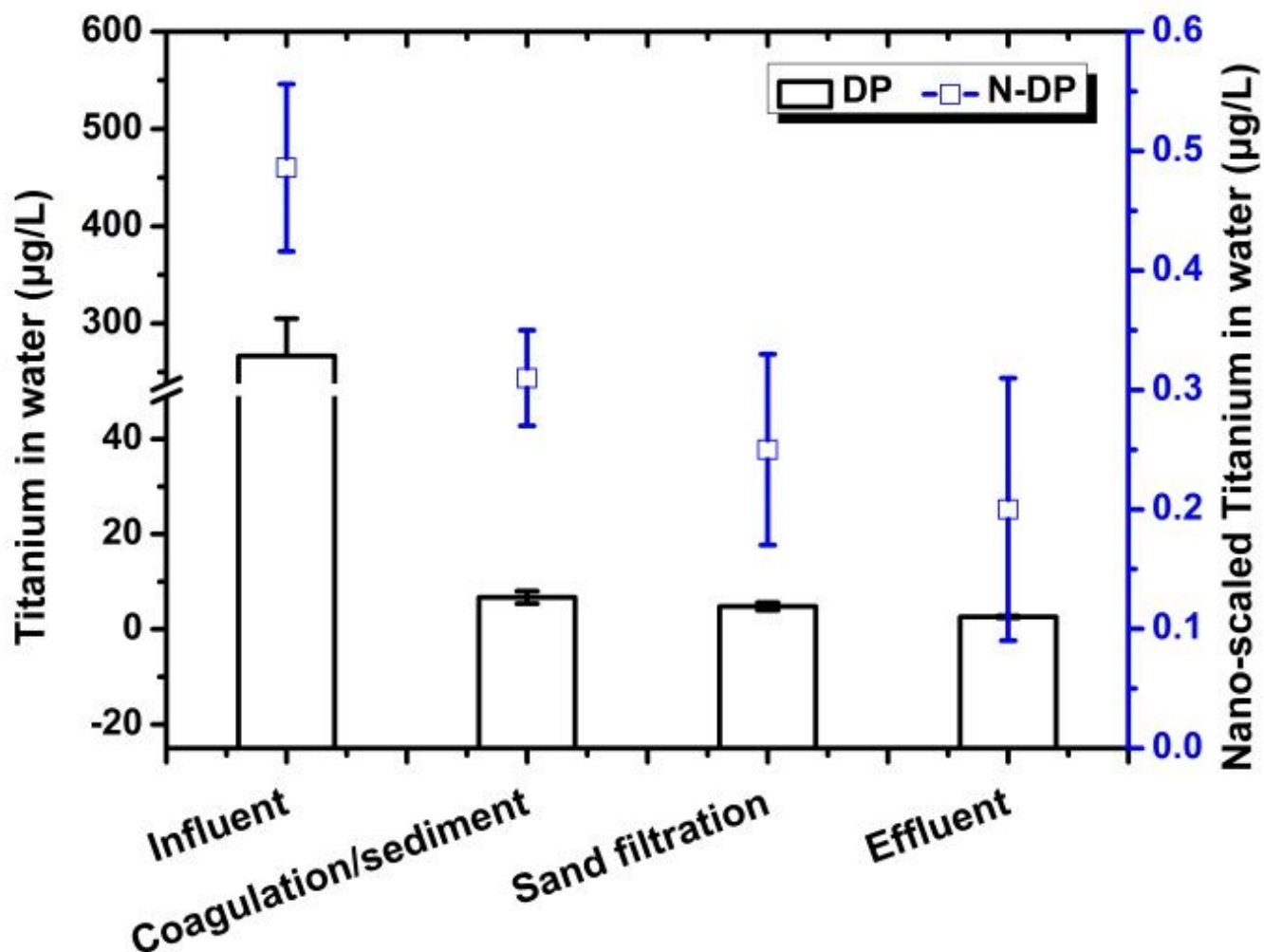


Figure 5

Removal performance of Ti (left y-axis) and nano-scaled Ti (right y-axis) in the representative water samples collected after various stages at the drinking water treatment plant. DP and N-DP represent the total Ti and nano-scaled Ti in the samples collected from the drinking water treatment plant, respectively.

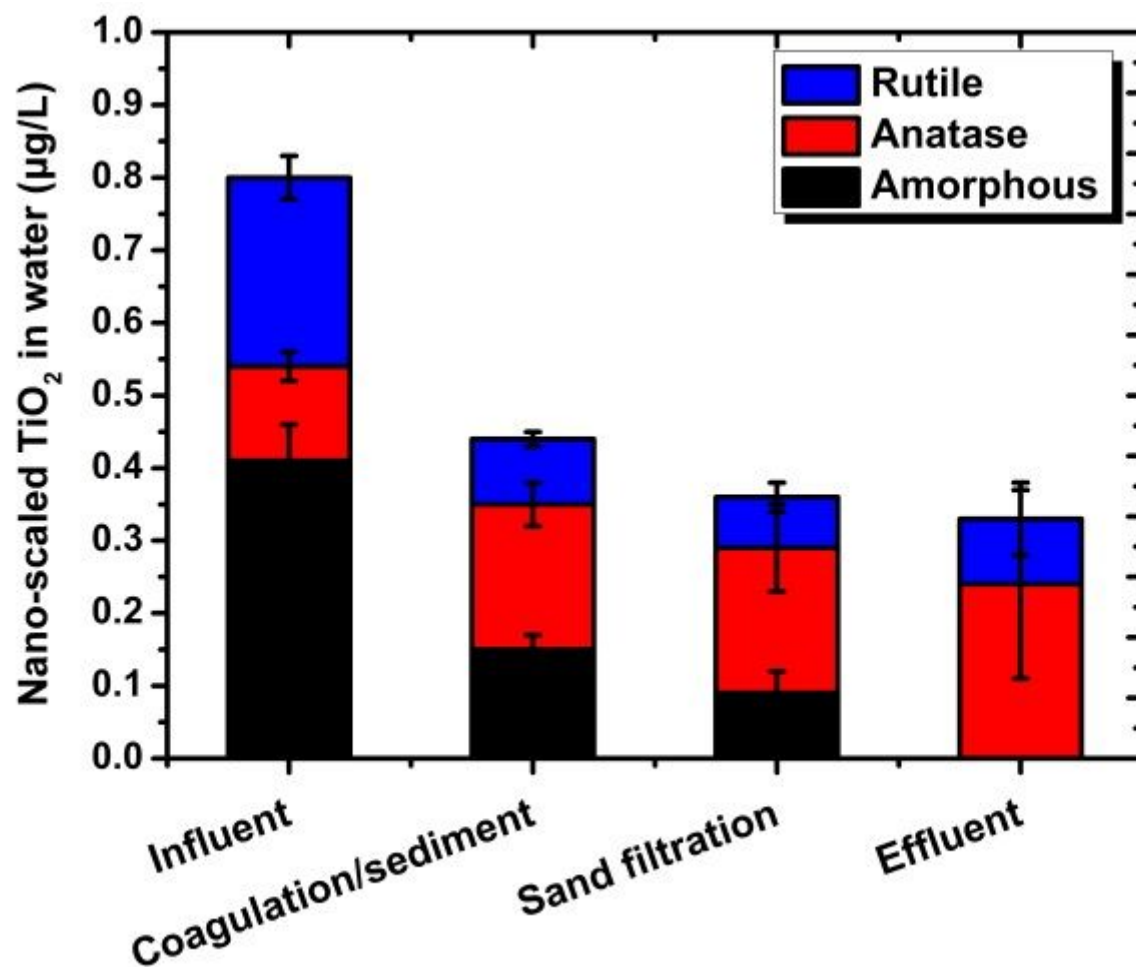


Figure 6

Crystal compositions of the representative water samples collected from the effluent of various stages at the drinking water plant.

Supplementary Files

This is a list of supplementary files associated with this preprint. Click to download.

- [SupportinginformationESP.docx](#)